AJEV | American Journal of Enology and Viticulture

Research Report
DOI: 10.5344/ajev.2023.23069

Hydrogen Sulfide Formation in Canned Wines: Variation Among Can Sources

Matthew J. Sheehan [1], Jose Hector R. Suarez,[1] Megan M. Benefeito,[1] Julie M. Goddard [1], and Gavin L. Sacks [1]*

Abstract

Background and goals

Wines packaged in aluminum beverage cans accumulate more hydrogen sulfide (H_2S, rotten egg aroma) than wines in glass, likely due to the reaction of aluminum with sulfites (SO_2). This work evaluated the variability of H_2S formation as a function of molecular and free SO_2 among commercial can liners and potential causes for observed differences.

Methods and key findings

Five commercial wines were adjusted to varying free SO_2, molecular SO_2, and pH, and packaged for up to eight months in cans with three different liners (one bisphenol A [BPA] epoxy and two BPA–non-intent [BPA-NI] epoxy). Molecular SO_2 was the best predictor of H_2S formation following long-term storage. Although visible corrosion was greater in the can neck, H_2S formation required direct contact between aluminum and wine. In follow-up accelerated aging studies using 10 liner sources representing five manufacturers, considerable variation in H_2S production was observed, even among cans with the same liner chemistry. Unused cans were characterized by range of optical, physical, and electrochemical techniques. An inverse correlation was observed between liner thickness and H_2S production, but the poor predictive ability of other techniques suggested that differences among liners were brought about because of the reaction of the liner and wine during storage.

Conclusions and significance

H_2S formation during storage of canned wines with high molecular SO_2 shows considerable variation among can manufacturers, even for similar liner chemistries. Assessment of liner appropriateness for canned wine should involve storage of the wine under accelerated or long-term conditions.

Key words: aluminum beverage can, BPA, canned wine, polymeric liner, sulfites, sulfur-like off-aroma

Introduction

The global market for canned wines in 2021 was $235.7 million USD (in revenue) and is expected to rise to $571.8 million by 2028 (Grand View Research 2021), nearly a 30-fold increase from 2014 ($2 million in revenue) (Weed 2019). The expected increase in popularity of canned wines is attributed to several reasons including their convenience, lightweight design, ruggedness, established recycling channels, and acceptance at venues where glass is prohibited such as stadiums, festivals, and pools (Jacoby 2019, Ruggeri et al. 2022, US EPA 2023).

As with other types of wine packaging, wine producers are concerned with potential effects of aluminum beverage cans on wine quality. Aluminum (Al^0) readily corrodes in the presence of oxygen or water to generate a passive layer of oxidized aluminum (Al^{3+}, e.g., Al_2O_3). In the absence of a coating, and at the low pH typical of wines and other beverages (pH <4), this passive oxide layer would dissolve (Robertson 2013), leading to an increase in dissolved Al^{3+} and eventually package leaking and loss of the hermetic seal (Robertson 2013). To mitigate corrosion, a thin polymeric coating (also called a "liner", "varnish", or "lacquer") is applied to the inside of aluminum beverage cans (Robertson 2013). Until recently, nearly all beverage can liners were bisphenol A (BPA)-based epoxies, the "gold-standard" liner material since the 1950s because of their inertness, low cost, and excellent barrier properties (LaKind 2013, Geueke 2016). However, because of concerns regarding BPA's role as a potential endocrine disruptor, its use has been curtailed in recent years, either through explicit bans (as occurred in France in 2015) (Geueke 2016) or by requirements that the presence of BPA must be declared on the label (as is the case in California since 2016). Alternative beverage can liners (also referred to as "bisphenol A-non-intent," or "BPA-NI,") have become more widespread in recent years, including those based on older materials such as acrylic (LaKind 2013), and newer epoxies based on monomers with lower endocrine activity than BPA (e.g., tetramethyl bisphenol F) (Szafran et al. 2017).

[1]Department of Food Science, Cornell University, Ithaca, NY 14853.
*Corresponding author (gls9@cornell.edu)
Submitted Oct 2023, accepted Dec 2023, published Feb 2024

Despite the presence of a liner, there is good evidence that canned wine may react with an aluminum beverage can to generate hydrogen sulfide (H_2S, "rotten egg" aroma, ~1 µg/L odor threshold) (Allison et al. 2021). Recent work demonstrated that glass packaged commercial wines developed only trace levels of H_2S (<6 µg/L, and typically undetectable) after eight months, but that the same wines could produce high levels of H_2S (>1000 µg/L) when stored in acrylic lined cans (Montgomery et al. 2023). Suprathreshold H_2S concentrations (up to ~50 µg/L) were also observed in BPA epoxy and BPA-NI epoxy cans (Allison and Sacks 2021, Montgomery et al. 2023). Across wines, the best predictor of H_2S accumulation during can storage was the initial concentration of molecular SO_2; similar results were observed under accelerated aging conditions using lined aluminum coupons. Free SO_2 and pH were also well-correlated with H_2S production, but other factors (i.e., total SO_2, chloride, copper, and alcohol) were poorly correlated with H_2S production (Montgomery et al. 2023). Based on these results, H_2S formation was hypothesized to occur through the following reaction (Allison et al. 2021, Montgomery et al. 2023):

$$2\ Al^0_{(s)} + SO_{2\ (aq)} + 6\ H^+_{(aq)} \rightarrow 2\ Al^{3+}_{(aq)} + H_2S_{(g)} + 2\ H_2O \quad \text{(Eq. 1)}$$

Because wines that produced high H_2S also showed signs of liner degradation, it was speculated that SO_2 either directly damaged the liner or else was able to diffuse through the liner to generate H_2S gas and induce delamination.

Earlier work evaluated liners sourced from a single can manufacturer; variation in H_2S formation among can manufacturers with similar liner chemistries was not considered (Montgomery et al. 2023). We hypothesized that H_2S formation during long-term storage in canned wines would vary among can manufacturers even for the same liner type. We further hypothesized that variation in H_2S among can manufacturers for the same liner type could be explained by differences in the can composition and the consistency of the liner application, which could be evaluated by employing a range of tools to characterize can and liner properties.

Materials and Methods

Materials and chemical reagents

Acetaldehyde (99%), potassium metabisulfite ($K_2S_2O_5$, 99%; "KMBS"), copper sulfate (99%), and sodium chloride (99%) were from Alfa Aesar, Chem Products, Sigma-Aldrich, and Calbiochem, respectively. Sulfuric acid (25% v/v) and potassium carbonate (≥99%; K_2CO_3) were made by BDH Chemicals and were obtained from VWR. Deionized, distilled water with a resistance of 18.2 MΩ • cm at 25°C was produced using a Milli-Q system (Millipore Sigma) and was used for all experiments.

Nitrogen liquid and gas (N_2, Ultra High Purity) cylinders were supplied by Airgas USA LLC. A 500 mL liquid nitrogen (LN_2) sprayer was obtained from US Solid. Headspace vials (30 mm × 60 mm, 27 mL), 20 mm butyl rubber septa, 20 mm tear-away crimp seals, and a 20 mm hand crimper were all obtained from Supelco (product codes 27298, Z166065, 27016, and 33280-U, respectively). A 5 to 25 mL bottle-top dispenser was obtained from VWR (product code 82017-768). A coated, clear 1000 mL glass bottle with septa port was obtained from Ankom Technology. A Surebonder (FPC Corporation) electric glue skillet and ethyl vinyl acetate (EVA) hot glue pellets (B-2001; Surebonder – FPC Corp.) were obtained through Amazon.

Industry collaborators provided 0.24 mm thick sheets of 3004 aluminum alloy coated with BPA-NI epoxy on both sides (~2 µm-thick liner), 355 mL aluminum beverage can bodies (202D/211 standard, 202/204 × 604 sleek), and can ends (5000 series alloy, BPA Epoxy 202LOE B64 style). The commercially available coatings on the can bodies were BPA epoxy, BPA-NI epoxy, and acrylic (2 to 5 µm coating thickness); uncoated aluminum cans were also provided. An Oktober MK16 can seamer was obtained from Oktober Design.

Commercial wines and initial chemical analysis

Five commercial wines were generously donated by an industry cooperator in 20-L high-density polyethylene KeyKegs: Pinot grigio (PG), Sauvignon blanc (SB), French rosé (FR), sparkling rosé (RB), and sparkling white (WB). Details on the wine style, vintage, and basic wine chemistry are provided in Supplemental Table 1. Basic wine chemistry was determined by established methods at the Cornell Craft Beverage Analytical Laboratory (Geneva, NY). Briefly, alcohol by volume (ABV) was analyzed using a Foss OenoFoss, free SO_2 analysis was carried out by flow injection analysis on a Foss FIAstar 5000 Analyzer, titratable acidity (TA) was measured by titration with 0.1 N sodium hydroxide to pH 8.2 endpoint with a Metrohm 862 Compact titrator and a Hanna Instruments HI901W automatic titrator, and pH was measured on a Fisher Scientific Accumet Excel XL25 dual-channel pH/ion meter.

Molecular SO_2 was calculated from Equation 2 using acid dissociation constant values (pK_a) adjusted for alcohol as described by Coelho et al. (2015):

$$\text{Molecular } SO_2 = \frac{\text{Free } SO_2}{1+10^{\text{pH}-\text{pKa}}} \quad \text{(Eq. 2)}$$

The aluminum content in the wines was determined by a local facility (USDA-ARS Holley Center) using a Thermo Scientific iCAP 6500 series system for inductively coupled plasma-atomic emission spectroscopy; the protocol is described elsewhere (Zhou et al. 2016). Initial H_2S was measured by gas detection tubes, as described below.

Canning procedure

Cans were filled with wine directly from the KeyKegs using the supplied KeyKeg manual pump. After filling, a few drops of LN_2 were added to sparge the headspace of O_2, and the can was immediately topped with a lid and seamed on a manual double seamer (MK16 seamer; Oktober Design). Seam quality was validated using a standard industry protocol consisting of measuring the seam thicknesses at four different points (first operation, second operation, cover hook, body hook) at three locations around the seam (Oktober Design 2024). Prior to the canning experiments, total package oxygen (TPO, or the sum of liquid and headspace O_2, normalized against volume) was measured as described elsewhere using model wine (Montgomery et al. 2023). For TPO measurements, O_2 in the can headspace and liquid were equilibrated by gently agitating for one hour. The can was then opened, and dissolved O_2 in the liquid was measured by a Fibox 3 LCD trace O_2 meter fitted with a DP-PSt6 O_2 dipping probe (PreSens). The headspace O_2 content could then be calculated from the headspace volume and literature value for O_2 volatility; the TPO was calculated based on the sum of headspace and dissolved O_2, and was determined to be <1.5 mg O_2/L for the tested cans.

H_2S in canned wines over long-term storage as a function of pH and SO_2

To evaluate the effects of pH, free SO_2, and molecular SO_2 on H_2S production in canned wine, five wines (PG, SB, FR, RB, and WB) were prepared in three groups prior to canning:

1. Low molecular SO_2, low free SO_2 – Control group, no adjustments
2. Low molecular SO_2, high free SO_2 – KMBS added, pH adjusted to 3.65 to 3.80 with K_2CO_3
3. High molecular SO_2, high free SO_2 – KMBS added, no pH adjustment

Following adjustments, the low and high free SO_2 values ranged from 15 to 20 and 40 to 50 mg/L, respectively. The low and high molecular SO_2 values ranged from 0.6 to 1.1 and 1.5 to 2.5 mg/L, respectively. The pH values ranged from 3.11 to 3.37 for the wines without pH adjustment, and from 3.65 to 3.80 for the wines with K_2CO_3 added. The pH was adjusted in Group 2 so the free SO_2 was similar to that of Group 3.

Wines were canned as described above in one of three can types: BPA epoxy (Company X), BPA-NI epoxy (Company Y), and BPA-NI epoxy (Company Z), then stored at 20°C in an upright position away from sun and light, until analysis at four and eight months of storage. Three can replicates were prepared for each wine (n = 5), composition (n = 3), can type (n = 3), and time point (n = 2), for a total of 270 individual can samples. The H_2S in each sample was measured at the appropriate time point.

Accelerated aging – preparation of aluminum coupons and testing protocol

Preparation of coupons was based on an approach described and validated elsewhere (Montgomery et al. 2023). Can tops and bottoms were removed with a Gryphon C-40 band saw (Gryphon Corp.), then cut vertically with scissors to open the body (Supplemental Figure 1). Rectangular coupons (1 cm × 4 cm total) were cut by stainless steel shears from the middle of the side of the can body, and two 1 cm × 2 cm coupons were prepared from the headspace region of the can body (Supplemental Figure 2A to 2C) for each accelerated aging trial to maintain a constant surface-to-volume ratio in the 27 mL vial. The bare, uncoated edges were then sealed with EVA hot melt glue.

Accelerated aging trials were performed as described by Montgomery et al. (2023). Bottled or kegged wine was transferred into an ethanol-sanitized 20-L plastic water cooler, previously sanitized by a 70% ethanol rinse. Prior to filling, wines were nitrogen-purged until dissolved O_2 was <0.1 mg/L by PreSens Fibox 3 LCD trace O_2 meter with DP-PSt6 O_2 dipping probe. During vial filling, nitrogen was used to backfill the cooler to limit O_2 pickup. For each accelerated test, a 27-mL glass crimp-top vial was purged with two to three drops of LN_2 before rapidly adding deoxygenated wine (25 mL) and a coated, edge-sealed aluminum coupon. A butyl rubber septum was then placed on top of the vial, but not sealed, to allow excess LN_2 to dissipate (10 to 15 sec), after which the vials were sealed with a 20-mm aluminum metal crimp cap. Accelerated aging took place at 50°C prior to H_2S measurement after three and 14 days. This protocol achieved O_2 pickup of <0.5 mg/L O_2, as determined by the PreSens meter (Montgomery et al. 2023); measurements on model solutions indicated that there was a negligible amount of O_2 ingress over three and 14 days of storage in-vial.

H_2S production under accelerated conditions: can source, can liner type, and within-can location

To evaluate variation in H_2S production across commercial cans, 10 can types (three BPA epoxy, five BPA-NI epoxy, two acrylic) were sourced from a total of five commercial suppliers (designated V, W, X, Y, and Z). The cans were coded with letters V to Z, signifying the can producer, followed by 1 (BPA epoxy), 2 (BPA-NI epoxy), or 3 (acrylic), to signify the liner type. For two of the can sources, multiple production batches (n = 2 or 3) were tested to evaluate batch-to-batch variation. For example, X1 and X1-2 indicate two batches of BPA epoxy cans from manufacturer X. Y2-2 was observed to have incomplete liner coverage based on visual inspection. Y2-3 was the same liner material as Y2, but had a thinner layer of liner material applied. A high molecular SO_2 commercial 2020 German Riesling (pH 3.1, molecular SO_2 = 2.56 mg/L, free SO_2 = 43 mg/L, ABV = 9.3%) was used for accelerated aging trials. Accelerated aging trials took place for both three or 14 days, because earlier work had demonstrated that the average of three day and

14 day trials was most predictive of long term aging, and all treatments (can type × location in can × timepoint) were prepared in triplicate.

H_2S production by immersed and non-immersed regions of aluminum

To evaluate if immersed and non-immersed regions of aluminum produced similar H_2S concentrations, a modified accelerated aging experiment was developed. Coupons were prepared from BPA-NI epoxy coated Al 3004 sheets as described above. For each accelerated aging test, coated coupons were inserted in one of four orientations (Supplemental Figure 3):

1. One coupon (4 cm × 1 cm) was fully submerged, and a second coupon (1 cm × 1 cm) was bonded to hot melt glue on the underside of the vial septa in the vial headspace.
2. A single coupon (5 cm × 1 cm) was partially submerged, with ~1 cm^2 exposed to the vapor phase.
3. One coupon (4 cm × 1 cm) was fully submerged, and a second coupon (1 cm × 1 cm) was also fully submerged.
4. A single coupon (1 cm × 1 cm) was glued to the underside of the vial septa in the vial headspace, with ~1 cm^2 exposed to the vapor phase.

H_2S quantification

H_2S was measured by colorimetric gas detection tubes (GDT) attached to a commercial aeration-oxidation (A-O) apparatus, described in more detail elsewhere (Allison et al. 2021). An H_2S selective GDT (4LT and 4LL tubes; Gastec International) was inserted between the receiver flask of an A-O apparatus (GW Kent, Inc.) and the vacuum source. Aspiration of a wine sample resulted in staining of the GDT tube via reaction of H_2S with a metal salt; the stain length was proportional to the original H_2S concentration. Interferences from SO_2 were prevented by inserting an SO_2 selective GDT (Gastec 5L) between the H_2S GDT and A-O unit. The method detection limit was previously reported to be ~1 µg/L (Allison et al. 2021).

Characterization of polymeric liner and aluminum interior surface of cans

The interiors of the cans used in the long-term storage trials (X1, Y2, and Z2) were evaluated both before and after storage by several optical and spectroscopic techniques. For some techniques, unlined cans provided by the manufacturers were also analyzed as described below. To prepare the flat sections of cans for evaluation, cans were cut across the body with a Gryphon C-40 bandsaw (Gryphon Corp.), then cut vertically with scissors to open the body, as described for coupon preparation. For post-storage cans, a seam teardown tool (Oktober Design) was used to first remove the can lid. Samples were obtained from five different vertical locations along each can, as shown in Figure 1. Coupons were 0.25 cm × 0.25 cm, except for coupons from the can headspace, where smaller coupons (~0.25 cm × 0.1 cm) were used because larger, flat samples could not be prepared. Elemental composition of unused bare aluminum cans and pre- and post-storage lined cans were determined by x-ray fluorescence (XRF) (Bruker Tracer III-SD). Samples (1 cm × 1 cm) were prepared (Figure 1, Location 4) and run in triplicate, with the voltage set to 40 kV, current set to 40 µA, and a 60 sec dwell time. The portable device was mounted in the upward facing tabletop geometry and samples were placed on the measurement window with the inner face of the can sample pointing toward the window for data collection. XRF peak areas were fit using PyMCA (Solé et al. 2007).

Liner composition was characterized by Fourier transform infrared-attenuated total reflectance (FTIR-ATR) on a Bruker Vertex V80V Vacuum FTIR system (Cornell Center for Materials Research [CCMR], Ithaca, NY) in a nitrogen atmosphere. For FTIR analyses, coupons (0.5 cm × 0.5 cm) were prepared in triplicate from the middle of the can body (Figure 1, Location 4). Spectra were collected from 4000 to 700 cm^{-1} (Sultanova et al. 2019).

For profiling liner thickness and aluminum uniformity, laser-scanning profilometry was performed at the CCMR using a Keyence VK-X260 laser-scanning profilometer. Each

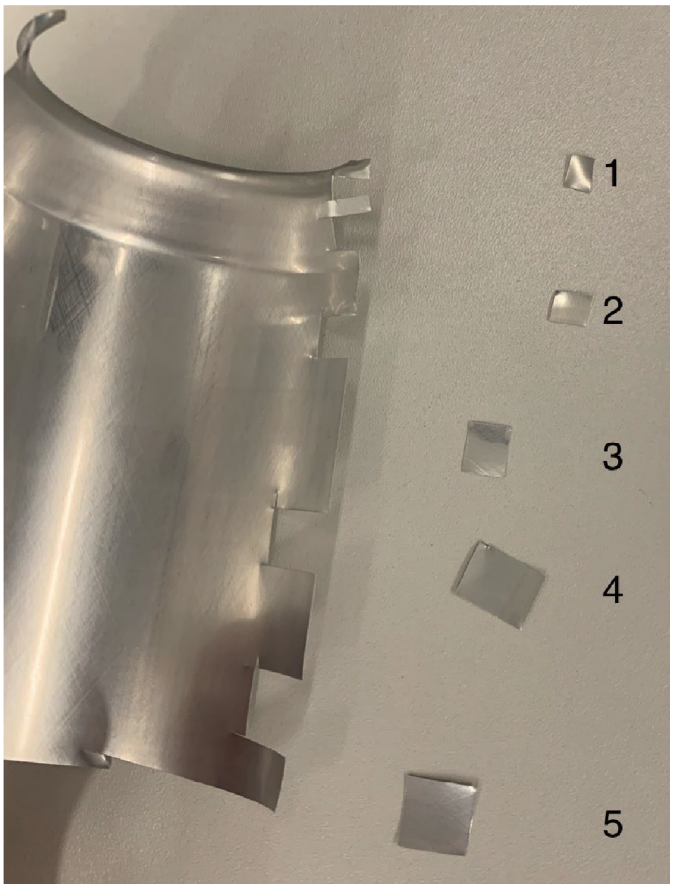

Figure 1 Locations within can body sampled for liner and aluminum surface analysis: 1, top of neck, adjacent to seam; 2, tapered portion of can neck; 3, upper can body below the neck; 4, middle can body; and 5, lower can body.

sample was analyzed at 408 nm using the surface profile feature to study the aluminum surface uniformity and the thin film feature to study liner thickness and uniformity. For the thin film analysis, a refractive index of 1.7 was used for BPA and BPA-NI epoxy liners based on the literature value for polycarbonate (Sultanova et al. 2019) in the range of 435 to 1052 nm and extrapolating to 408 nm. The measurement size for a sample was roughly 285 µm × 210 µm.

Liner thickness in the body and bottom (dome) of the can was also evaluated by optical interferometry (SpecMetrix ACS-10 Model, Sensory Analytics LLC) (Komaragiri and Telep 2017). A broad range of wavelengths (700 to 1400 nm) was used and a refractive index of 1.55 was chosen for analysis. Three cans of each type were sampled for analysis.

To characterize liner integrity (e.g., the presence of pores), electrochemical impedance spectroscopy (EIS) was performed on cans in triplicate using a PalmSens3 potentiostat and PSTrace 5.9 software. Intact, unused lined cans were evaluated in place of coupons using protocols described elsewhere (Esteves et al. 2014, Daroonparvar et al. 2021). The setup is shown in Supplemental Figure 4 and is similar to aluminum can EIS measurements described by Grandle and Taylor (1994). Briefly, can bottom exteriors were sanded with 1000 grit sandpaper (Dura-Gold), washed with 70% ethanol, and dried to ensure a clean aluminum surface contact with the working electrode. The cans were filled with sodium chloride (NaCl) electrolyte solution (35 g/L), and a counter electrode (flat cell steel) and reference electrode (silver/silver chloride, potassium chloride as reference electrolyte) were inserted into the electrolyte solution and placed inside a Faraday cage to avoid external electromagnetic interferences. For the working electrode, electrical contact was made with the bottom of the can. The open circuit potential (OCP) was allowed to stabilize (drift <0.01 ΔmV/sec) before measurements were taken; the parameters used for OCP and EIS are shown in Supplemental Tables 2 and 3. For metal exposure measurements, a WACO Enamel Rater III was obtained, and a 10 g/L NaCl electrolyte solution was used to evaluate the three can types from the long-term aging study. A constant electrolyte fill level was maintained across all the cans, and the stainless steel electrode was placed into the can for measurement. The industry standard test was used, which consists of applying 6.3 V for 4 sec before measuring the current.

Liner adhesion quality was evaluated by an industry standard method, ASTM D3359-17 (Test Method B), using Scotch Bi-Directional Filament Tape 8959 (180° peel strength of 11 N/cm) on unused cans (ASTM 2022): six parallel horizontal and six parallel vertical cuts are made on the interior of the can, and pressure-sensitive tape is applied to that area. After 90 sec, the tape is removed and the percentage of the area with removed liner is determined.

The presence of uncoated regions on cans was evaluated qualitatively by ASBC Can Method 8 (ASBC 2011). An aqueous solution of hydrochloric acid (0.027 N) and copper sulfate pentahydrate (100 g/L) was added to cans (n = 3 replicates) and stored at room temperature for 45 min. Uncoated regions could be detected by the presence of Cu deposits, as described (ASBC 2011).

Statistical analysis and software

Statistical analysis was done via JMP Pro 16 and JMP Pro 17 (SAS Institute, Inc.). Analysis of variance (ANOVA; $\alpha = 0.05$) was used to evaluate the effects of storage time, liner, and wine composition on H_2S production. A p value of <0.05 was used to determine significant differences among treatment groups.

Results and Discussion

H_2S in canned wines with varying liner sources and composition over long-term storage

Using a wine adjusted to varying pH and SO_2 concentrations, previous work demonstrated that H_2S formation in the presence of aluminum coupons was higher for acrylic liners than for epoxy liners, and that H_2S was best correlated with molecular SO_2 rather than free SO_2 or pH. However, this earlier work was performed on a single wine, single liner type, and was not validated with long-term storage conditions (Montgomery et al. 2023).

To confirm that molecular SO_2, but not free SO_2, best predicts H_2S production across a broader range of cans and wine sources, five commercial wines were adjusted with K_2CO_3 and SO_2 to yield three treatments per wine:

I. Low pH, low free SO_2, low molecular SO_2
II. High pH, high free SO_2, low molecular SO_2
III. Low pH, high free SO_2, high molecular SO_2

Other hypothetical combinations, e.g., low pH, high free SO_2, and low molecular SO_2, could not be generated because molecular SO_2 is dependent on the free SO_2 and hydrogen ion concentration ($[H^+]$). However, these treatments were sufficient for decoupling the relative importance of these three factors. The "high" molecular SO_2 range was 1.6 to 2.6 mg/L. Although this range is high compared to typical molecular SO_2 recommendations to prevent microbial spoilage (0.5 to 0.8 mg/L) (Zoecklein et al. 1999), the molecular SO_2 values in this paper were calculated using ethanol-adjusted pK_a values, and "conventional" molecular SO_2 values based on the pK_a of water will underestimate molecular SO_2 by 25 to 50% (Coelho et al. 2015). Thus, this range is equivalent to 0.8 to 2.0 mg/L molecular SO_2 based on conventional calculations.

The unadjusted Treatment I wines contained undetectable H_2S except for trace levels (<3 µg/L) in the RB wine. H_2S was not measured in the wines immediately following pH and/or SO_2 adjustment (Treatments II and III), but was assumed to be unchanged. Wines were then stored in cans from three different manufacturers (X1 = BPA epoxy, Y2 and Z2 = BPA-NI epoxy) and H_2S was measured after four and eight months of storage (Figure 2). In the unadjusted wines (Treatment I), average H_2S was below sensory threshold (<10 µg/L) in all five wines at both four and eight month time points. Interestingly, no correlation was observed between

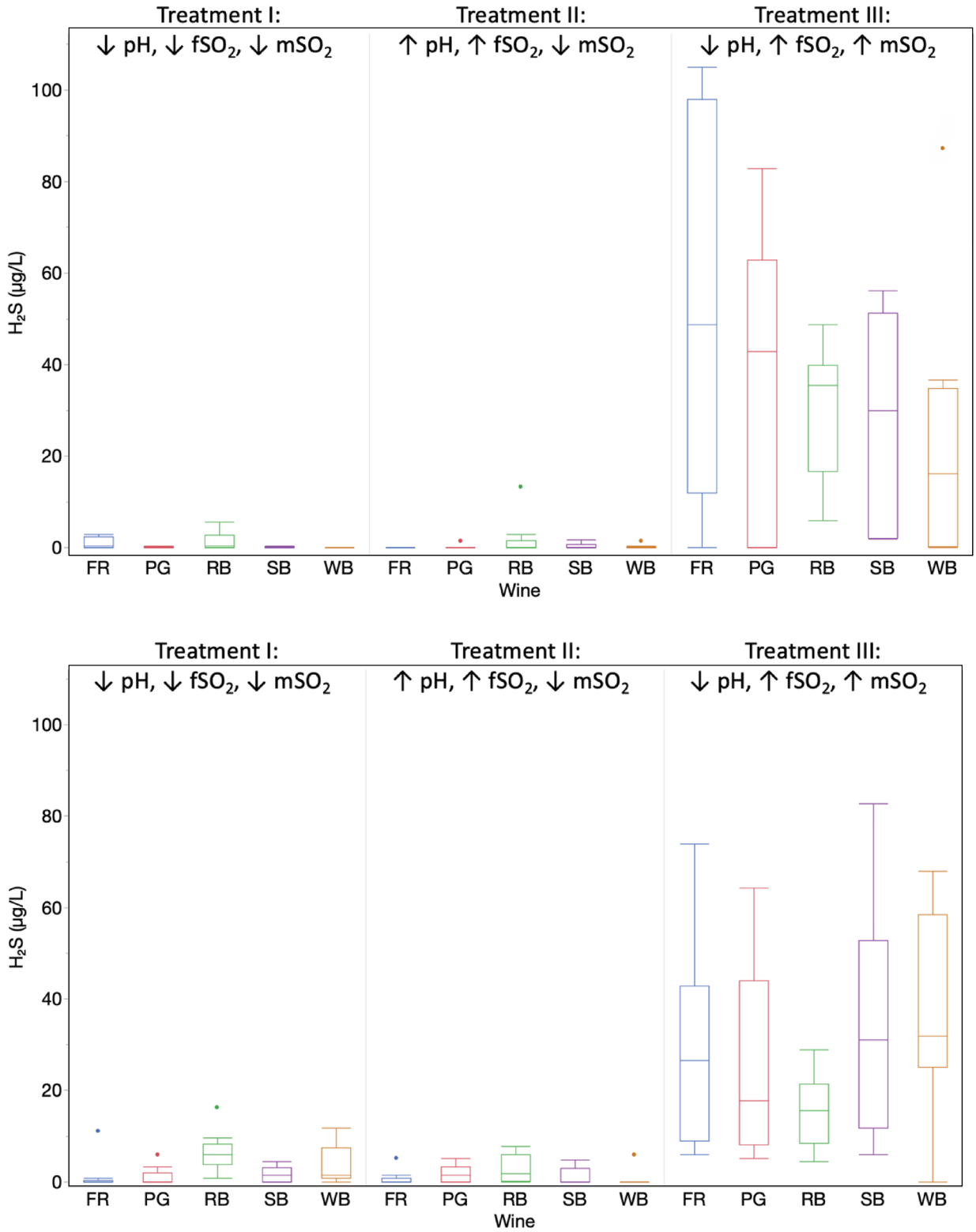

Figure 2 Hydrogen sulfide (H_2S) production by treatment group and wine after four months (top) and eight months (bottom). Boxes represent range of H_2S produced across three can liners, stored in duplicate (n = 6 points for each time point, wine, and treatment). ↓ pH, ↓ fSO_2, and ↓ mSO_2, low pH, low free SO_2, and low molecular SO_2, respectively; ↑ pH, ↑ fSO_2, and ↑ mSO_2, high pH, high free SO_2, and high molecular SO_2, respectively. FR, French rosé; PG, Pinot grigio; RB, bubbly rosé; SB, Sauvignon blanc; WB, white bubbly.

molecular SO_2 and H_2S concentration in the adjusted wines, in contrast to an earlier report (Montgomery et al. 2023). Potentially, this is because the range of molecular SO_2 values in the current study (0.59 to 1.07 mg/L) was considerably smaller than the range of the earlier work (0.13 to 2.4 mg/L).

H_2S was notably higher in Treatment III than in Treatment II or Treatment I (ANOVA, $p < 0.05$). For Treatment III, the average H_2S formed after four months was 28.7 µg/L, with some samples producing >100 µg/L H_2S (Figure 2, top). By comparison, H_2S formation in Treatment I and II wines averaged 2.2 µg/L (Figure 2, top). Similar differences were observed after eight months of product storage (Figure 2, bottom), which also showed that higher H_2S formation is formed in the presence of high molecular SO_2 (Treatment III), and not by free SO_2 alone (Treatment II), in agreement with previous observations under accelerated aging conditions with a single wine and liner source (Montgomery et al. 2023). All H_2S concentrations—particularly for Treatment III—were higher than those observed in bottled wine (≤6 µg/L) as well as the H_2S sensory threshold (~1 µg/L) (Allison et al. 2021). Previously, it was speculated that the neutral molecular SO_2 would be able to diffuse through the nonpolar liners to react with the metal surface. However, as molecular SO_2 is a component of free SO_2 and its proportional contribution will be favored at low pH, it is thus not possible to distinguish the effect of molecular SO_2 from the interaction of [free SO_2] × [H^+]. No significant correlation was observed between H_2S accumulation and any of the other wine parameters (alcohol, TA, dissolved aluminum, residual sugar) reported in Supplemental Table 1 (one-way ANOVA, $p > 0.05$ for all tests).

The long-term aging study also allowed for comparison of H_2S production across can liners for different wines. Results for Treatment III wines stored in the three liners are shown in Figure 3. Z2 cans produced lower H_2S (average = 5.9 µg/L ± 2.1) than the same wines stored in X1 or Y2 cans (average = 36.6 ug/L ± 3.2), as shown in Figure 3 (two-way ANOVA, $p < 0.05$). These differences are notable because Y2 and Z2 reportedly use the same liner material (Valspar V70) and differ only in their manufacturers. Furthermore, Z2 produced less H_2S than X1, even though the latter used BPA epoxy, a liner typically considered to be the "gold standard" for beverage cans. Additionally, Can Z2 wines also had significantly lower variance than either Can X1 or Can Y2 wines (Levene's test, $p < 0.05$). Previous work on canned wines also reported high variation in H_2S production among can replicates (relative standard deviation >50%); all cans in the previous study were from the same can manufacturer, and it was not possible to determine if variation arose from sample preparation, analytical characterization, or can-to-can differences (Montgomery et al. 2023). Other authors have noted that can-to-can variability may be a considerable source of variation in beverage can corrosion, potentially due to variation in liner thickness or cure quality (Grandle and Taylor 1997, Folle et al. 2008, Soares et al. 2019). This current work suggests this may also be important for explaining variation in H_2S production; the specific role of liner thickness is discussed in greater detail later.

X1 cans produced the most H_2S in the low SO_2 (Treatment I) control wines (ANOVA, $p = 0.029$; data not shown), and the amount of H_2S in the Treatment I control group rose for each liner, from four to eight months (Figure 2).

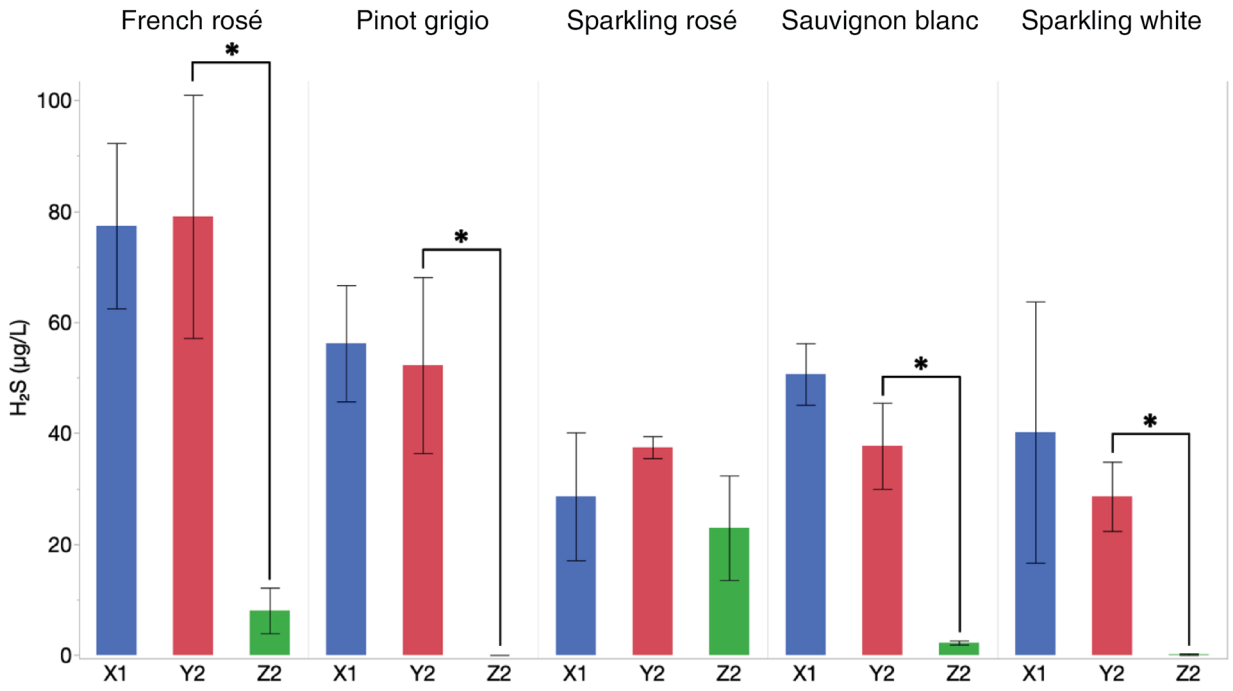

Figure 3 Hydrogen sulfide (H_2S) production by liner (X1, Y2, and Z2) for each of the five Treatment III (high molecular SO_2) wines after four months of storage. Error bars represent one standard error of three technical replicates. The asterisks indicate $p < 0.05$ (analysis of variance). X1, Y2, Z2: X, Y, and Z signify the can manufacturer; 1 and 2 signify the liner type (BPA epoxy and BPA-NI epoxy, respectively). For example, Y2 indicates a BPA-NI epoxy can from manufacturer Y.

H_2S production from can headspace versus body

Previous work demonstrated that cans with higher amounts of H_2S formation following long-term storage also had greater visible corrosion (Montgomery et al. 2023). Visible corrosion was not scored in the current study. However, we observed that the location of visible corrosion varied among can sources. Can X1 had visible corrosion mostly in the body of the can, with lesser amounts in the neck region of the can (not shown), but Y2 had considerable corrosion in the upper neck region (Supplemental Figure 5B).

To evaluate if the neck and body regions of a can had different susceptibility to corrosion, coupons were created from the headspace region of the neck (Figure 1, Locations 1 and 2) and the side walls of the body (Figure 1, Location 4) and were incubated in a commercial Riesling under accelerated conditions (three days at 50°C). The resulting H_2S concentrations are shown in Figure 4. H_2S production was highest for the headspace neck region of Y2, approximately three-fold higher than the body region, which agrees with the observed differences in visible corrosion. However, because the surface area of the body is ten-fold greater than the neck, these differences are not likely to explain differences in overall performance among can manufacturers.

To determine if H_2S production was greater in non-immersed regions, an accelerated aging trial was performed with the location of aluminum coupon varied. Negligible H_2S production was observed when aluminum was present only in the headspace, indicating that H_2S generation (Equation 1) requires contact with the wine. Additionally, no increased visible corrosion or H_2S production was observed when the coupon was fully immersed (Treatment III) versus partially immersed (Treatments I and II), as shown in Figure 5. Thus, the visible corrosion observed for Can Y2 is likely because the coating in this region is providing a less effective barrier (see Figure 4), and not because corrosion is accelerated in non-immersed regions, as compared to immersed regions.

H_2S production during accelerated aging of lined aluminum coupons from multiple manufacturers

To further characterize the variation in H_2S production among can manufacturers for similar liner types, accelerated aging testing was conducted with coupons produced from cans used in the long-term study discussed above (i.e., X1, Y2, and Z2), along with seven other liners, for a total of 10 liner treatments. For these experiments, a single, commercially available German Riesling with high molecular SO_2 was used.

H_2S production under accelerated conditions across liners is shown (Figure 6). In agreement with previous work (Montgomery et al. 2023), acrylic liners generated much higher amounts of H_2S (up to 100 µg/L) than the other liner types, with the exception of Y2-2 (Figure 6; Tukey test, p

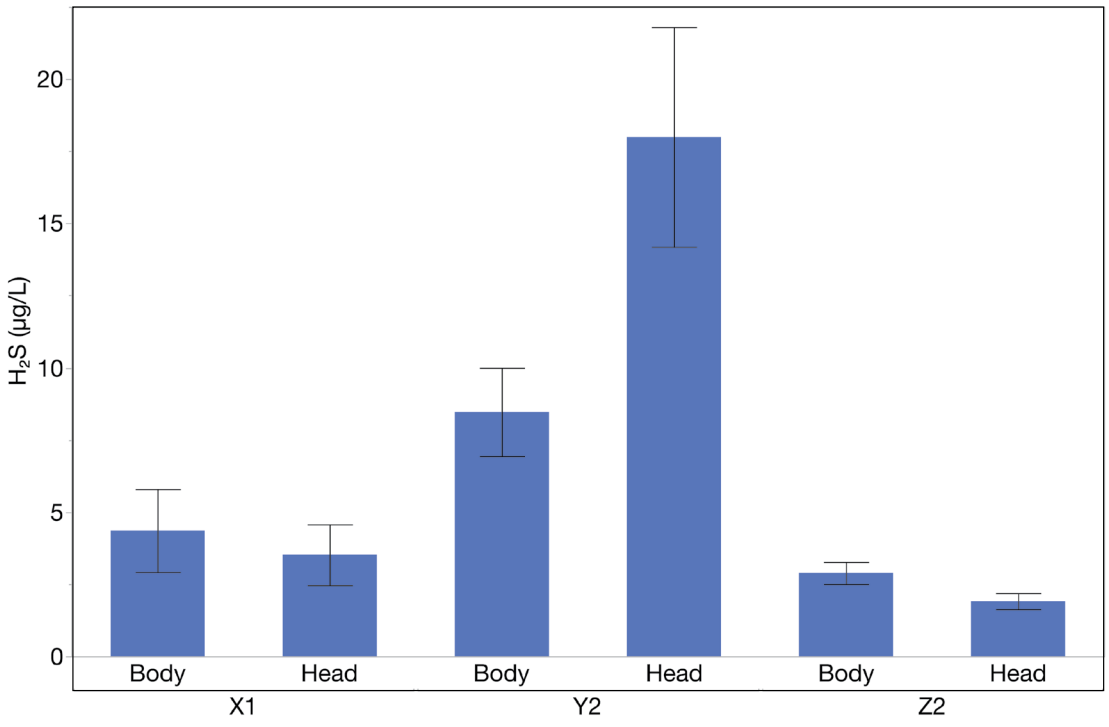

Figure 4 Hydrogen sulfide (H_2S) production from can body (see Figure 1, Location 4) and headspace (see Figure 1, Locations 1 and 2) coupons from three different batches of cans (X1, Y2, and Z2), using the accelerated aging assay in triplicate (technical replicates), measuring at three and 14 days of storage. A negative control (no coupon) produced 0.5 µg/L H_2S. Error bars represent one standard error. X1, Y2, Z2: X, Y, and Z signify the can manufacturer; 1 and 2 signify the liner type (BPA epoxy and BPA-NI epoxy, respectively). For example, Y2 indicates a BPA-NI epoxy can from manufacturer Y.

< 0.05). As with long-term aging, differences in H_2S formation were observed among can manufacturers even for the same liner type. For example, Z2 produced less H_2S than all three batches of Y2 (ANOVA, $p < 0.05$), and Z1 produced less H_2S than X1 (ANOVA, $p < 0.05$). Similarly, there were significant differences in H_2S production among acrylic coatings from different producers (Y3, W3), as well as significantly higher variation in H_2S (Levene's test, $p < 0.05$). Finally, batch-to-batch variation was observed among Y2 cans, with approximately ten-fold higher H_2S production in the visually defective batch (Y2-2) than in either the original batch (Y2) or thinner liner cans (Y2-3). The Y2-2 cans had clear visible defects in the moat of the can (see Supplemental Figure 6), which likely accounted for their poor performance.

Polymeric liner and aluminum surface characterization

Earlier work demonstrated that liner type critically affects H_2S production during canned wine storage, with wines stored in the presence of acrylic liners forming greater than ten-fold more H_2S than epoxy liners (Montgomery et al. 2023). However, both long-term and accelerated aging results of the current work showed that comparable variation can occur among cans with the same liner types sourced from different manufacturers.

For the three can sources used in the long-term study (X1, Y2, and Z2), variation in performance (both average H_2S formation and can-to-can variation) was hypothesized to have arisen from one, or a combination, of aluminum alloy composition, polymeric liner composition, liner degree of cure, and liner thickness and uniformity.

Aluminum alloy composition

The aluminum alloy compositions of cans from BPA-NI epoxy producers Y and Z were determined by XRF spectrometry and are shown in Supplemental Figure 7. These two cans were selected because they used the same liner chemistry. The results are semiquantitative, because calibration curves were not run. The only element to show variation >20% among can sources was chromium (Cr), which was approximately three-fold higher in Z. Considering the low typical concentrations of Cr in the Al 3004 alloy (<0.05%) (United Aluminum 2023), variation in this element appeared unlikely to explain differences in H_2S formation. Other transition metals detected in the alloys, especially Cu (in its soluble Cu(II) form), are well-known to form nonvolatile complexes or polysulfides following reaction with H_2S, and could potentially limit accumulation of H_2S if solubilized (Kreitman et al. 2019). However, variation in Cu and other elements (beyond Cr) were minor (<20%) and unlikely to explain the observed differences in H_2S accumulation.

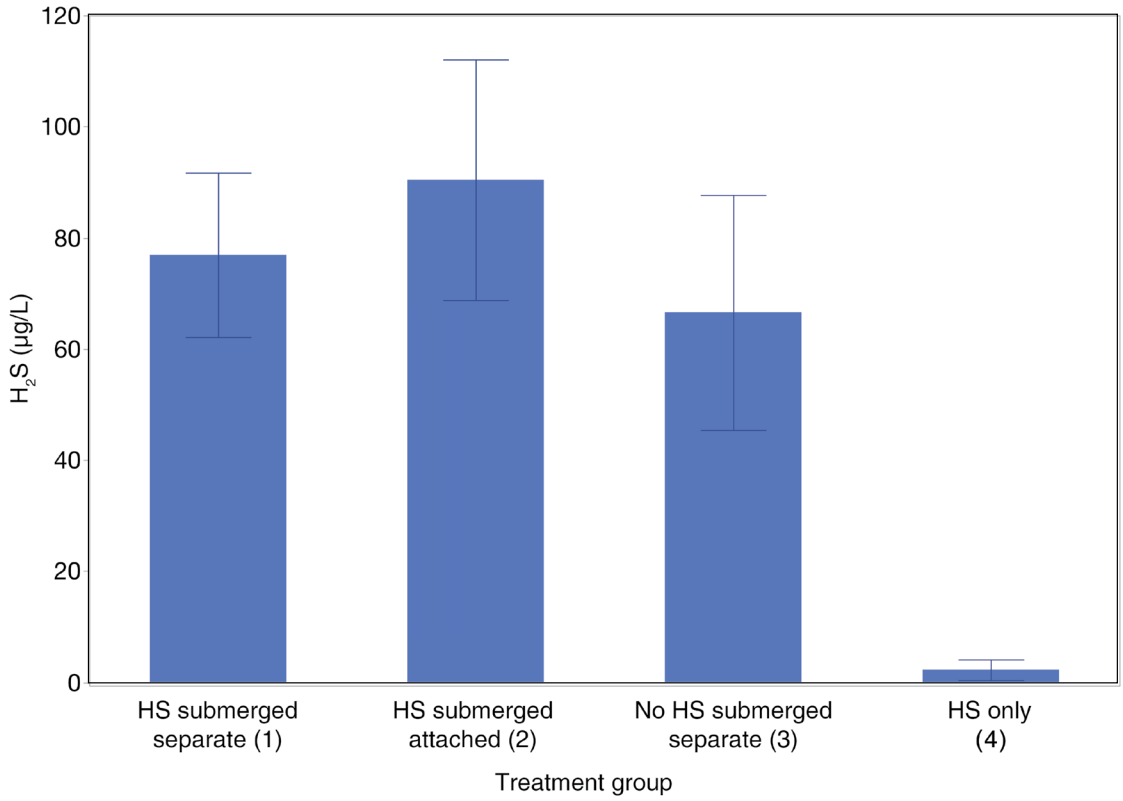

Figure 5 Dependence of hydrogen sulfide (H_2S) formation on location of coated aluminum coupon (headspace [HS] versus immersed). Treatment 1, two coupons, one in headspace and one immersed; Treatment 2, one intact coupon, partially in headspace and partially immersed; Treatment 3, two coupons, both immersed; and Treatment 4, coupon in HS only. Three technical replicates were tested for each treatment. Error bars represent one standard error. A negative control group produced 0.5 µg/L H_2S.

Liner composition by FTIR-ATR

Liners of cans used in the long-term storage experiment were characterized by FTIR, and spectra are shown in Supplemental Figure 8. Minor differences were seen between BPA epoxy (Can X) and the two BPA-NI epoxy (Cans Y2 and Z2) cans, but the liner used in Y2 and Z2 cans showed no visible differences. This latter result was expected because literature from the producers indicated both liners were Valspar V70 (tetramethyl bisphenol F) based coatings. Significant peaks were observed at ~1725, 1510, 1210, 1140, and 1030 cm^{-1}.

Aluminum surface smoothness, liner thickness, and liner uniformity

Enamel rating, EIS, copper sulfate rinses, and liner adhesion tests were performed to evaluate liner integrity. Metal exposure analysis ("enamel rating") uses two electrodes: one on the can exterior and one immersed in an electrolyte solution contained within the can. Application of a direct current (DC) potential (6.3 V) results in an electrical current (in milliamps [mA]) proportional to the extent of exposed aluminum (Sencon 2019). Manufacturers that use enamel ratings typically have quality control cutoffs based on the corrosivity of the beverage; for beer, a noncorrosive beverage, the recommended cutoff is 75 mA (Fetters et al. 2004), but a lower cutoff (5 mA) is recommended for highly corrosive beverages like wine (personal communication with an anonymous industry member). In this study, enamel rating currents were not significantly different among the three groups of cans used in the long-term aging study, and all measured values were <4 mA (Supplemental Figure 9). We attempted to evaluate the enamel rating approach by testing the previously mentioned Y2-2 cans with obvious visual defects in liner coverage within the "moat" of the can (Supplemental Figure 6). Surprisingly, only two of the 15 cans failed the enamel rater test, as indicated by the presence of a short-circuit, with the others having ratings <1.5 mA. This may be due to the formation of a thicker, nonconductive Al_2O_3 layer on the exposed areas between the time of can manufacturing and their laboratory evaluation. At the least, these results suggest that enamel rating may not be as useful for end users (e.g., wineries) as they would be for can manufacturers.

EIS is similar to enamel rating except that an alternating current (AC) potential is applied instead of DC potential, and the resulting data modeled as one of several possible equivalent circuits (Lazanas and Prodromidis 2023). In our work, the EIS data was modeled as a resistor-capacitor (RC) circuit, and the impedance at low frequency (0.05 Hz) was evaluated because it is reported to correlate well with poststorage visual can corrosion and coating performance in a model corrosive beverage (3.5% NaCl, adjusted to pH 3

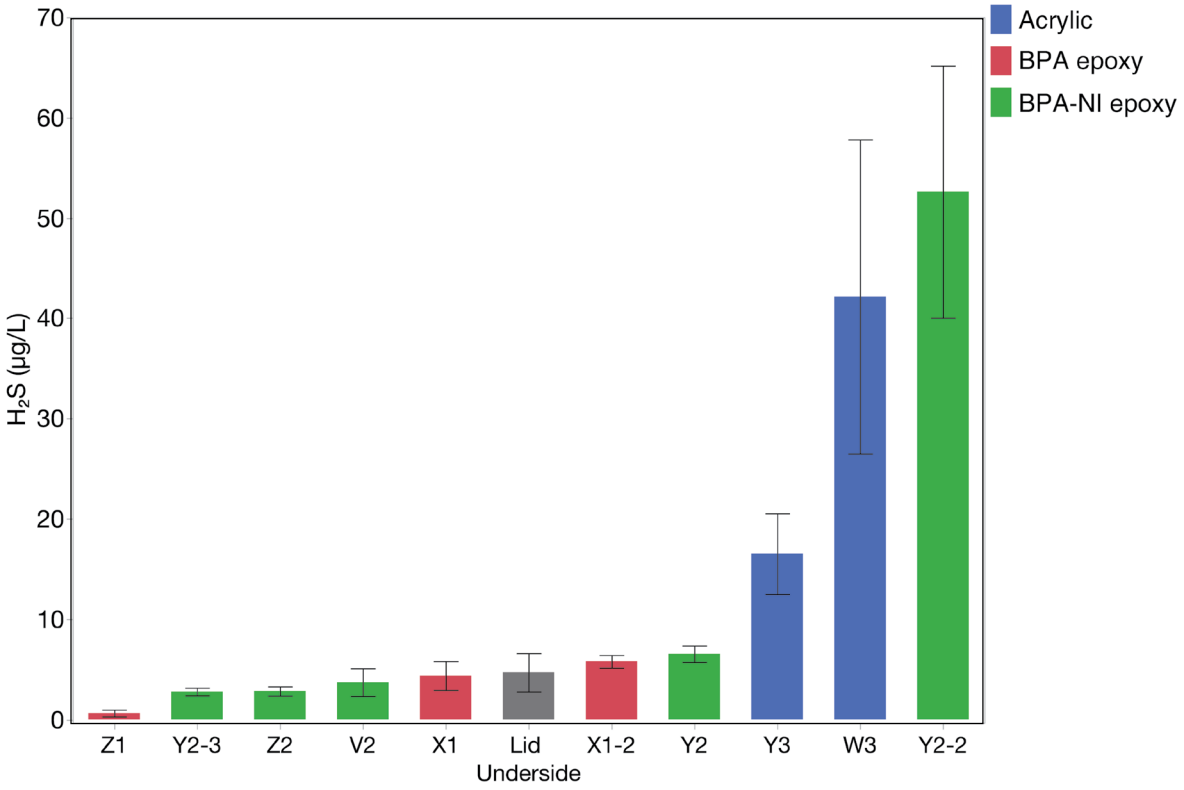

Figure 6 Hydrogen sulfide (H_2S) production for 10 different can types, as well as the underside of the can lid, after three days in accelerated aging conditions with a commercial German Riesling. Three technical replicates for each type of can (represented on the x-axis) were tested. Error bars represent one standard error. The cans were coded with letters V to Z, signifying the can manufacturer, followed by 1 (BPA epoxy), 2 (BPA-NI epoxy), or 3 (acrylic), to signify the liner type. For two of the can sources, multiple production batches (n = 2 or 3) were tested to evaluate batch-to-batch variation (e.g., Y2-2 indicates it is the second batch of BPA-NI epoxy cans from manufacturer Y).

with acetic acid), as reported in Grandle and Taylor (1994). Average impedance values at 0.05 Hz were ~10 MΩ, which is above the minimum value recommended to limit corrosion (McIntyre and Pham 1996). However, no significant differences in either average values or variance were observed among the three can producers (Supplemental Figure 10). This observation was surprising because several reports have suggested that impedance values can be related to long-term can performance (Grandle and Taylor 1994, Kern et al. 1999, Hollaender 1997). One possible explanation is that the wine (especially the SO_2 in wine) degrades the liner during long-term storage—this behavior was highly evident visually for acrylic liners in previous work, and could also occur for epoxy-type liners (Montgomery et al. 2023). In the current study, EIS measurements were performed within one hour of filling, but other reports have suggested looking for changes in EIS data over a longer time course (out to 14 days) to observe evidence of liner degradation (Grandle and Taylor 1994, de Vooys et al. 2012, Lu et al. 2017). This was not attempted in the current work but would be appropriate for further study.

Treatment of unused cans from the long-term aging study with acidified copper sulfate resulted in no deposition of Cu onto the internal surface of the can or aluminum sulfate precipitation, indicating that there were no voids in the liner of sufficient size to be apparent to the naked eye, i.e., <0.05 mm (data not shown). To validate the test, the Y2-2 cans with visual defects were also evaluated, but no displacement reaction could be observed. As with the enamel rating tests, considerable time may have passed between can manufacturing and liner testing, allowing for formation of a protective oxide layer. Similarly, no material was removed by the ASTM D3359-17 adhesion test (data not shown).

Liner thickness values were determined by performing laser scanning profilometry and analyzing a uniformly coated subsection of the aluminum (Table 1). The Z2 cans had a significantly thicker liner (3.27 µm ± 0.37 µm) than the Y2 cans (2.96 µm ± 0.35 µm). The liner thickness of X1 was intermediary (3.01 µm ± 0.43 µm) and did not differ from Cans Y and Z (Student's t-test, Figure 7). The observation that Z2 cans had slightly (~10%) higher average liner thickness than the other cans could be a potential explanation for the better performance of Z2 cans. However, based on profilometry, these same Z2 cans also had an initially higher proportion of exposed aluminum and thin liner coverage (<0.5 µm), as shown in Table 1. Thus, these latter parameters are presumably not responsible for the lower levels of H_2S observed in Z cans.

Manufacturer Z's BPA epoxy and manufacturer V's BPA-NI epoxy, both slim cans, produced very little H_2S in the accelerated aging protocol (Figure 6) and had significantly thicker liners (Figure 7), despite a larger internal surface area, than the rest of the 10 liners analyzed (Student's t-tests, $p < 0.05$).

A regression of inverse liner thickness versus H_2S produced is shown in Figure 8, with acrylic liners and the defective Y2-2 cans excluded. The rate of SO_2 permeation and thus, H_2S formation, was assumed to be proportional to the inverse of the liner thickness, and significant correlation was observed between the inverse of liner thickness and H_2S. Additionally, the two liners that produced the least amount of H_2S (Figure 6, Y2-3 and Z1) had the lowest liner thickness standard deviations (Figure 7), suggesting that a lack of variation in liner thickness (and not just average liner thickness) was important for minimizing H_2S. Interestingly, the cans with the thinnest liner, Y2-3, produced intermediate amounts of H_2S. All the cans studied, except for Y2-3, were slated for "hard-to-hold," beverages such as kombuchas, sour beer, wine, energy drinks, and ready-to-drink beverages, meaning a greater amount of liner was applied to the can, and more strict quality control checks (Enamel Rater, manufacturer-specific tests) were met than for typical cans. The Y2-3 cans are a "soda-weight" or "beer-weight" can with a smaller amount of liner applied, and a lower cure temperature, than cans for "hard-to-hold" products.

Although Company Y's acrylic liner (Y3) was the thickest measured (Figure 7), high H_2S was also observed for this liner. Previous work demonstrated that SO_2 will degrade acrylic liners, resulting in more exposed aluminum and likely explaining the much higher levels of H_2S observed in acrylic-lined cans (Montgomery et al. 2023).

Liner thickness was also evaluated by interferometry. This technique reports average liner thickness values for multiple 1 to 2 mm^2 areas within a can, but finer resolution at the micron level (as was performed with profilometry) was not available. Summary statistics for the three can sources used in long-term studies are reported (Table 2). The order of thickness (Z>X>Y) for both average and minimum values in the can body was the same as the order measured with profilometry.

The liner thickness on the underside of can ends, which rarely show visual signs of corrosion, was measured by examining a flat portion. The average thickness of can ends was >8 µm, roughly three-fold thicker than the can bodies.

Table 1 Percentage of sample surface area at different liner thickness cutoffs. The percentages are averages of three technical replicates. Samples were taken from Locations 1 to 5 as shown in Figure 1. X1, Y2, Z2: X, Y, and Z signify the can manufacturer; 1 and 2 signify the liner type (BPA epoxy and BPA-NI epoxy, respectively). For two of the can sources, multiple production batches (n = 2 or 3) were tested to evaluate batch-to-batch variation (e.g., Y2-3 indicates the third batch of BPA-NI epoxy cans from manufacturer Y).

	Liner thickness (µm)				
% Surface area	**0**	**<0.01**	**<0.5**	**<1**	**<1.5**
X1	2.0%	3.1%	13.3%	17.0%	19.5%
Y2	2.6%	4.4%	17.7%	21.5%	24.7%
Z2	2.5%	5.6%	22.0%	26.5%	30.2%
	Liner thickness (µm)				
% Surface area	**0**	**<0.01**	**<0.5**	**<1**	**<1.5**
Y2-3	3.2%	5.6%	25.9%	31.0%	35.3%

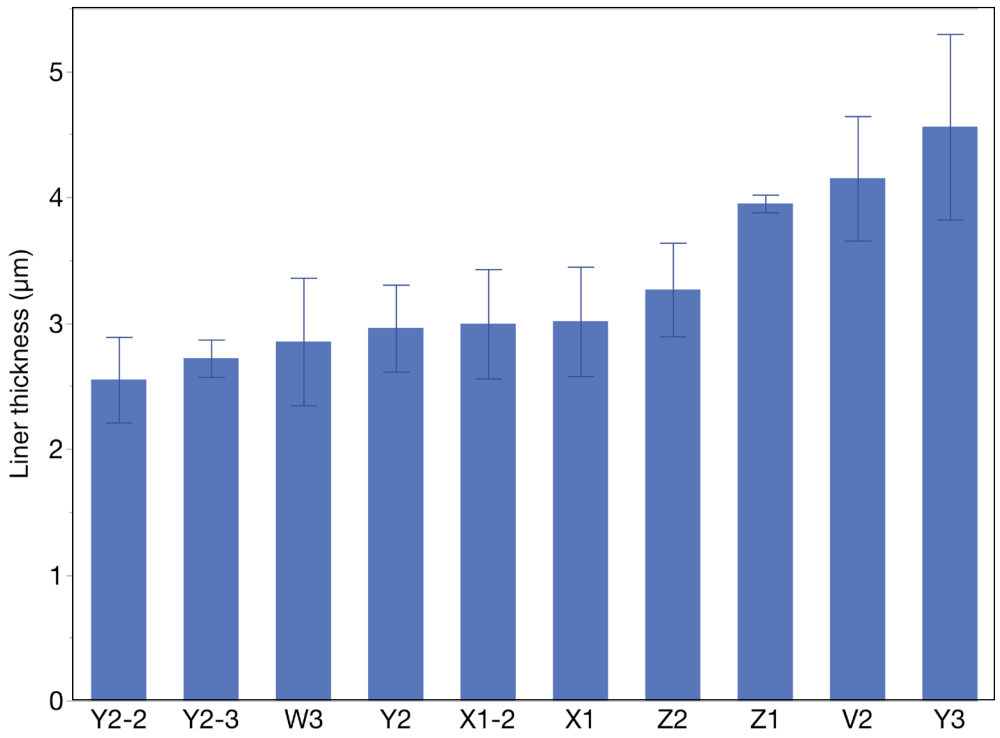

Figure 7 Can body liner thickness from 10 different can types, as measured by laser-scanning profilometer (n = 3 cans per liner type). Error bars represent one standard deviation. The cans were coded with letters V to Z, signifying the can manufacturer, followed by 1 (BPA epoxy), 2 (BPA-NI epoxy), or 3 (acrylic), to signify the liner type. For two of the can sources, multiple production batches (n = 2 or 3) were tested to evaluate batch-to-batch variation (e.g., Y2-2 indicates it is the second batch of BPA-NI epoxy cans from manufacturer Y).

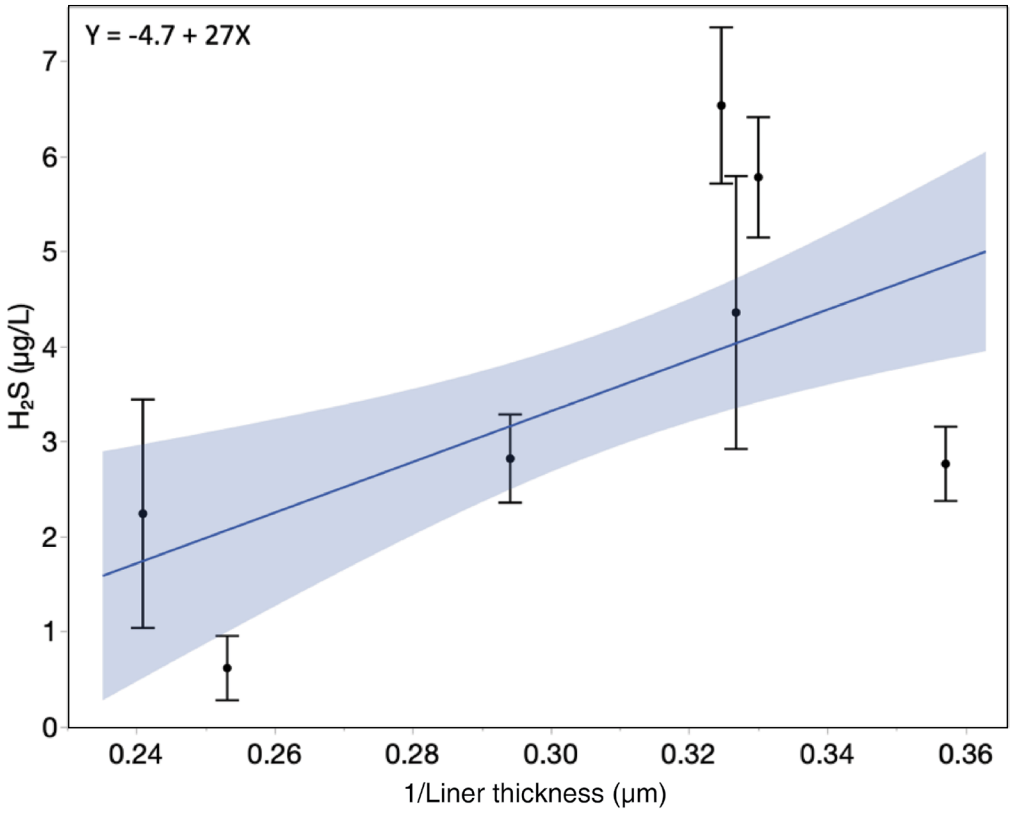

Figure 8 Hydrogen sulfide (H_2S) formation after three days at 50°C versus inverse liner thickness for epoxy lined cans (BPA and BPA-NI). Each point represents the average H_2S for a different liner (n = 8 technical replicates per liner). Error bars represent one standard error.

Table 2 Liner thicknesses (in µm) measured by laser interferometry for X1, Y2, and Z2 cans. Values are averages of multiple 1 to 2 mm^2 spots around the can interior. Four cans were analyzed at 24 spots in the can body and eight spots in the dome of each can. X1, Y2, Z2: X, Y, and Z signify the can manufacturer; 1 and 2 signify the liner type (BPA epoxy and BPA-NI epoxy, respectively). For example, Y2 indicates a BPA-NI epoxy can from manufacturer Y.

	Inside average	Minimum body	Maximum body	Dome average
X1	3.48	2.84	4.41	4.75
Y2	3.11	2.47	4.15	2.47
Z2	3.72	3.16	4.40	2.68

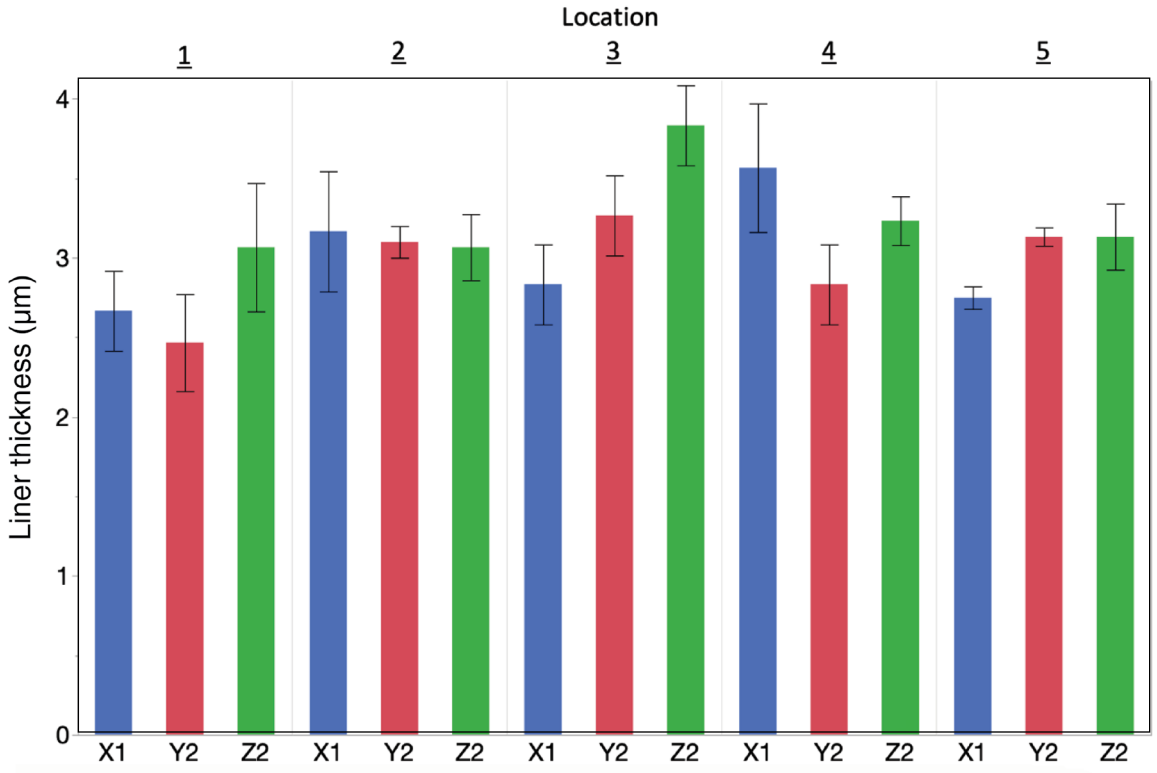

Figure 9 Liner thickness measurements by laser-scanning profilometry, measured across the cans (X1, Y2, and Z2). Three technical replicates were analyzed. Error bars represent one standard deviation. X1, Y2, Z2: X, Y, and Z signify the can manufacturer; 1 and 2 signify the liner type (BPA epoxy and BPA-NI epoxy, respectively). For example, Y2 indicates a BPA-NI epoxy can from manufacturer Y.

Liner thicknesses were also determined at five different locations throughout the can body and headspace for the three cans used in long-term aging studies. Measurements were performed by laser-scanning profilometry (Figure 1). The area of thinnest liner coverage (~2.5 µm) was in the top of the headspace (Location 1) of the Y2 cans (Figure 9). As reported above, the headspace of the Y2 cans generated more H_2S than any other can location, which further supports the hypothesis that thinner liners will typically have a shorter onset time before measurable H_2S production occurs, assuming all other factors are the same.

Conclusions

The molecular SO_2 fraction of sulfites was confirmed to be the best predictor of H_2S formation during storage of canned wines for a range of wines and can liners. Considerable variation in H_2S formation and visible corrosion occurs not only among different types of liner chemistry, but also for cans produced with the same liner material from different can manufacturers. Can-to-can variation was significantly higher for certain can manufacturers. Physical, optical, and mechanical tests of unused cans generally failed to predict performance during long-term storage, but differences in performance among cans were modestly correlated with differences in liner thickness. These observations, along with visible evidence of liner damage following storage, suggest that the chemical resistance of the liner to reactions with the wine (especially sulfites in wine), along with initial liner thickness, is critical to the stability of canned wines. The variation in liner performance identified in this work is likely to be relevant to other canned foods and beverages. Because the food or beverage may interact with the can liner, it is recommended to perform storage experiments with a can or coupon prior to evaluating the liner integrity.

Acknowledgments

Funding was provided by the New York Wine and Grape Foundation (NYWGF) and a gift from Archer Roose. Wines and cans were supplied by anonymous industry collaborators. This research was also supported in part by the intramural research program of the U.S. Department of Agriculture, National Institute of Food and Agriculture, Agriculture and Food Research Initiative program (accession number 2023-67017-39865). The findings and conclusions in this publication have not been formally disseminated by the U. S. Department of Agriculture and should not be construed to represent any agency determination or policy. The authors acknowledge SpecMetrix, Inc, for providing complementary analyses of can liners. The authors also acknowledge the use of facilities and instrumentation supported by NSF through the Cornell University Materials Research Science and Engineering Center DMR-1719875. This material is based on research sponsored by the Air Force Research Lab under agreement number FA8650-22-2-5200. The U.S. Government is authorized to reproduce and distribute reprints for Governmental purposes notwithstanding any copyright notation thereon.

Supplemental Data

The following supplemental materials are available for this article at ajevonline.org:

Supplemental Table 1 Initial composition of wines used in the long-term canning study. TA, titratable acidity; ABV, alcohol by volume.

Supplemental Table 2 Parameters for open circuit potential testing.

Supplemental Table 3 Parameters for electrochemical impedance spectroscopy testing. OCP, open circuit potential; DC, direct current; AC, alternating current.

Supplemental Figure 1 Can body with top and bottom removed.

Supplemental Figure 2 Locations of (**A**) body and (**B**) headspace coupons used for accelerated aging testing. Bare aluminum on the cut coupon edges was sealed with hot-melt glue prior to testing, as shown in (**C**).

Supplemental Figure 3 Experimental design for comparing effects of immersed and nonimmersed aluminum on hydrogen sulfide formation. Four technical replicates of each treatment were performed. HS, headspace.

Supplemental Figure 4 Electrochemical impedance spectroscopy setup with counter electrode on the left, reference electrode in the middle, and the working electrode contacting the bottom of the can. The electrochemical cell is placed inside a grounded Faraday cage.

Supplemental Figure 5 Unused can with no corrosion (left), and used can with visual corrosion in the neck region (right).

Supplemental Figure 6 Visual defects in the polymeric lining of the "moat," of Y2-2 cans prestorage. Y2-2, Y signifies the can manufacturer; 2 signifies the liner type (BPA-NI epoxy). For two of the can sources, multiple production batches (n = 2 or 3) were tested to evaluate batch-to-batch variation (e.g., Y2-2 indicates it is the second batch of BPA-NI epoxy cans from manufacturer Y).

Supplemental Figure 7 Elemental analysis by x-ray fluorescence (XRF) for Y2 and Z2 cans. Three technical replicates were analyzed. Y2 and Z2, Y and Z signify the can manufacturer; 2 signifies the liner type (BPA-NI epoxy). For example, Y2 indicates a BPA-NI epoxy can from manufacturer Y.

Supplemental Figure 8 Fourier transform infrared-attenuated total reflectance spectra of the three liners (on aluminum substrate) used in the long-term storage experiment (X1, Y2, and Z2). X1, Y2, Z2: X, Y, and Z signify the can manufacturer; 1 and 2 signify the liner type (BPA epoxy and BPA-NI epoxy, respectively). For example, Y2 indicates a BPA-NI epoxy can from manufacturer Y.

Supplemental Figure 9 Metal exposure ratings (enamel rating) for the three types of cans used in the long-term aging study (n = 48). X1, Y2, Z2: X, Y, and Z signify the can manufacturer; 1 and 2 signify the liner type (BPA epoxy and BPA-NI epoxy, respectively). For example, Y2 indicates a BPA-NI epoxy can from manufacturer Y.

Supplemental Figure 10 Impedance values at low-frequency (0.05 Hz) for the three can types used in the long-term aging study. Three technical replicates were tested for each can type (n = 9). Error bars represent one standard error. X1, Y2, Z2: X, Y, and Z signify the can manufacturer; 1 and 2 signify the liner type (BPA epoxy and BPA-NI epoxy, respectively). For example, Y2 indicates a BPA-NI epoxy can from manufacturer Y.

ORCID

Matthew J. Sheehan 0009-0005-2985-7344
Julie M. Goddard 0000-0002-3644-0732
Gavin L. Sacks 0000-0002-1403-0505

Citation

Sheehan MJ, Suarez JHR, Benefeito MM, Goddard JM and Sacks GL. 2024. Hydrogen sulfide formation in canned wines: Variation among can sources. Am J Enol Vitic 75:0750003. DOI: 10.5344/ajev.2023.23069

References

Allison RB and Sacks GL. 2021. Brine-releasable hydrogen sulfide in wine: Mechanism of release from copper complexes and effects of glutathione. J Agric Food Chem 69:13164-13172. DOI: 10.1021/acs.jafc.1c04885

Allison RB, Montgomery A and Sacks GL. 2021. Analysis of free hydrogen sulfide in wines using gas detection tubes. Catalyst 6:1-8. DOI: 10.5344/catalyst.2021.21003

American Society of Brewing Chemists (ASBC). 2011. Cans method 8. Copper sulfate test. *In* ASBC Methods of Analysis, online. American Society of Brewing Chemists, St. Paul, MN.

ASTM. 2022. Standard test methods for rating adhesion by tape test. D3359-17. *In* Book of Standards, 0601. ASTM International, West Conshohocken, PA. DOI: 10.1520/D3359-17

Coelho JM, Howe PA and Sacks GL. 2015. A headspace gas detection tube method to measure SO_2 in wine without disrupting SO_2 equilibria. Am J Enol Vitic 66:257-265. DOI: 10.5344/ajev.2015.14125

Daroonparvar M, Kasar AK, Farooq Khan MU, Menezes PL, Kay CM, Misra M et al. 2021. Improvement of wear, pitting corrosion resistance and repassivation ability of Mg-based alloys using high pressure cold sprayed (HPCS) commercially pure-titanium coatings. Coatings 11:57. DOI: 10.3390/coatings11010057

de Vooys ACA, Boelen B and van der Weijde DH. 2012. Screening of coated metal packaging cans using EIS. Prog Org Coat 73:202-210. DOI: 10.1016/j.porgcoat.2011.10.019

Esteves L, Garcia EM, Castro M das MR and Lins VFC. 2014. Electrochemical study of corrosion in aluminium cans in contact with soft drinks. Corros Eng Sci 49:665-668. DOI: 10.1179/1743278214y.0000000197

Fetters T, Brossia C, Frattiani A, Hopps J, Lawrence D, Rogers P et al. 2004. Evaluation of can packaging methods. J Am Sci Brew Chem 62:42-48. DOI: 10.1094/asbcj-62-0042

Folle LF, Silveira Netto SE and Schaeffer L. 2008. Analysis of the manufacturing process of beverage cans using aluminum alloy. J Mater Process Technol 205:347-352. DOI: 10.1016/j.jmatprotec.2007.11.249

Geueke B. 2016. FPF Dossier: Can coatings. Zenodo. DOI: 10.5281/zenodo.200633

Grand View Research. 2021. Canned Wine Market Size, Share & Trends Analysis Report by Product (Sparkling, Fortified), By Distribution Channel (Supermarket & Hypermarket, Online), By Region

(APAC, North America), And Segment Forecasts, 2021 - 2028. Vol. GVR-4-6803. San Francisco, CA. https://www.grandviewresearch.com/industry-analysis/canned-wines-market

Grandle JA and Taylor SR. 1994. Electrochemical impedance spectroscopy of coated aluminum beverage containers — Part 1: Determination of an optimal parameter for large sample evaluation. Corrosion 50:792-803. DOI: 10.5006/1.3293469

Grandle JA and Taylor SR. 1997. Electrochemical impedance spectroscopy as a method to evaluate coated aluminum beverage containers — Part 2: Statistical analysis of performance. Corrosion 53:347-355. DOI: 10.5006/1.3280477

Hollaender J. 1997. Rapid assessment of food/package interactions by electrochemical impedance spectroscopy (EIS). Food Addit Contam 14:617-626. DOI: 10.1080/02652039709374574

Jacoby M. 2019. Why glass recycling in the US is broken. Chem Eng News 97:28-32.

Kern P, Baner AL and Lange J. 1999. Electrochemical impedance spectroscopy as a tool for investigating the quality and performance of coated food cans. J Coat Technol 71:67-74. DOI: 10.1007/BF02697980

Komaragiri V and Telep D. 2017. New in process coating thickness measurement tools. http://www.specmetrix.com/wp-content/uploads/2017/09/AIMCAL_TechnicalPaper_Sensory_Window-Films.pdf

Kreitman GY, Elias RJ, Jeffery DW and Sacks GL. 2019. Loss and formation of malodorous volatile sulfhydryl compounds during wine storage. Crit Rev Food Sci Nutr 59:1728-1752. DOI: 10.1080/10408398.2018.1427043

LaKind JS. 2013. Can coatings for foods and beverages: Issues and options. Int J Tech Policy Manage 13:80-95. DOI: 10.1504/IJTPM.2013.050999

Lazanas AC and Prodromidis MI. 2023. Electrochemical impedance spectroscopy — A tutorial. ACS Meas Sci Au 3:162-193. DOI: 10.1021/acsmeasuresciau.2c00070

Lu F, Song B, He P, Wang Z and Wang J. 2017. Electrochemical impedance spectroscopy (EIS) study on the degradation of acrylic polyurethane coatings. RSC Adv 7:13742-13748. DOI: 10.1039/c6ra26341k

McIntyre JM and Pham HQ. 1996. Electrochemical impedance spectroscopy; a tool for organic coatings optimizations. Prog Org Coat 27:201-207. DOI: 10.1016/0300-9440(95)00532-3

Montgomery A, Allison RB, Goddard JM and Sacks GL. 2023. Hydrogen sulfide formation in canned wines under long-term and accelerated conditions. Am J Enol Vitic 74:0740011. DOI: 10.5344/ajev.2022.22051

Oktober Design. 2024. Can Seamer Operation Manual. Oktober Design, Grand Rapids, MI. https://drive.google.com/file/d/1RxReEpGaWBdFXCwyytRNC8FwuFkoppJ6/view

Robertson GL. 2013. Food Packaging Principles and Practice. 3d ed. CRC Press, Boca Raton, FL.

Ruggeri G, Mazzocchi C, Corsi S and Ranzenigo B. 2022. No more glass bottles? Canned wine and Italian consumers. Foods 11:1106. DOI: 10.3390/foods11081106

Sencon. 2019. Enamel Rating: Reference Guide - Version 1.0. Sencon Group. https://www.sencon.com/downloads/Enamel_Rating_Reference_Guide_v1.pdf

Soares DS, Bolgar G, Dantas ST, Augusto PED and Soares BMC. 2019. Interaction between aluminium cans and beverages: Influence of catalytic ions, alloy and coating in the corrosion process. Food Packag Shelf Life 19:56-65. DOI: 10.1016/j.fpsl.2018.11.012

Solé VA, Papillon E, Cotte M, Walter Ph and Susini J. 2007. A multiplatform code for the analysis of energy-dispersive X-ray fluorescence spectra. Spectrochim Acta Part B 62:63-68. DOI: 10.1016/j.sab.2006.12.002

Sultanova N, Kasarova S and I Nikolov. 2019. Refractive index considerations of polymers for optics. AIP Conf Proc 2075:030008. DOI: 10.1063/1.5091152

Szafran AT, Stossi F, Mancini MG, Walker CL and Mancini MA. 2017. Characterizing properties of non-estrogenic substituted bisphenol analogs using high throughput microscopy and image analysis. PLoS ONE 12:e0180141. DOI: 10.1371/journal.pone.0180141

United Aluminum. 2023. Aluminum Alloy 3004 Data Sheet and Properties. United Aluminum, North Haven, CT. https://unitedaluminum.com/aluminum-3004-alloy/

United States Environmental Protection Agency (US EPA). 2023. National Overview: Facts and Figures on Materials, Wastes and Recycling. https://www.epa.gov/facts-and-figures-about-materials-waste-and-recycling/national-overview-facts-and-figures-materials

Weed A. 2019. Canned wine comes of age. Wine Spectator. https://www.winespectator.com/articles/canned-wine-comes-of-age

Zhou S, Okekeogbu I, Sangireddy S, Ye Z, Li H, Bhatti S et al. 2016. Proteome modification in tomato plants upon long-term aluminum treatment. J Proteome Res 15:1670-1684. DOI: 10.1021/acs.jproteome.6b00128

Zoecklein BW, Fugelsang KC, Gump BH, and Nury FS. 1999. Wine Analysis and Production. Springer Science + Business Media, LLC, New York. DOI: 10.1007/978-1-4757-6967-8